VALIDATION OF OCEANSAT-2 SCATTEROMETER DATA

Ad Stoffelen and Anton Verhoef

KNMI, Royal Netherlands Meteorological Institute, De Bilt, the Netherlands

Abstract

The Oceansat 2 scatterometer backscatter and wind data have been evaluated. The backscatter data appear to be of good quality and only small calibration issues remain. The winds have been compared to ECMWF model and buoy winds. The ISRO wind data quality is reasonable, but does not yet meet the OSI SAF accuracy standards. Ad hoc calibration to mimic the SeaWinds backscatter PDF allows wind processing by well-tuned SeaWinds wind processing modules at KNMI and results in good winds above a few m/s. Correction of the backscatter processing at low backscatter values is expected to generally further improve low wind processing.

INTRODUCTION

On behalf of the European Meteorological Satellite Organisation (EUMETSAT) Ocean and Sea Ice (OSI) and Numerical Weather Prediction (NWP) Satellite Application Facilities (SAFs) KNMI coordinated an OceanSat-2 Cal/Val proposal answering to an Indian Space Research Organisation (ISRO) Announcement of Opportunity (AO) call (Stoffelen, 2008). Following the positive experiences with the application of ERS, QuikScat and ASCAT scatterometer winds, KNMI, ECMWF, IFREMER, the Met.Office of the UK, Meteo France and the Spanish CSIC defined a project to provide support in the calibration and validation phase of the scatterometer instrument, called OSCAT, onboard of the Oceansat-2 satellite. This satellite was successfully launched in September 2009 by ISRO and 8 months of level 2A (L2A) and level 2B (L2B) data were kindly provided to the Principle Investigator and ECMWF. The data have been evaluated at KNMI, ECMWF and IFREMER. Using the OSCAT Wind Data Processor (OWDP) prototype software that was developed in the scope of the NWP SAF, KNMI produced L2B OSCAT winds as well. Moreover, this software allows on-the-fly Quality Assurance (QA) and Quality Control with well-established methods, which are essential for automatic application of the winds in numerical applications, such as NWP. Both the ISRO L2A backscatter data and the ISRO L2B and OWDP computed winds have been analysed, as detailed below

TEST DATA AND PROCESSING METHOD

The ocean normalised radar backscatter cross section is a geophysical quantity, i.e., independent of the instrument measuring it. The OSCAT Ku-band radar wavelength is almost identical to the NASA SeaWinds scatterometer radar wavelength. Therefore, the SeaWinds Geophysical Model Function (GMF) should be applicable to OSCAT as well. Moreover, the measurement configurations of SeaWinds and OSCAT are very similar, such that the scientific developments on the SeaWinds wind Data Processor (SDP) will be applicable for OSCAT. The SDP winds have shown to provide superior buoy verification (Vogelzang et al., 2010). A first step to apply this processor is to map the OSCAT backscatter distribution onto the SeaWinds backscatter distribution, i.e., a calibration step. This step is also essential to extend the SeaWinds wind climate data record to the OSCAT era and is described below.

The work described in this report is based on a test data set provided by ISRO in August 2010. The data set contains L2A and L2B data in HDF5 (Padia, 2010) and covers the period of 5 November 2009 (2009 309) to 30 June 2010 (2010 181). The data have been created using ISRO processor version 1.2 (Attribute "Processor Version" in the HDF5 data files). The OSCAT Wind Data Processor (OWDP) was used to process the data and create L2B wind data in SeaWinds BUFR format (Leidner et al., 2000). The BUFR format is required by European users. OWDP uses the "genscat" software which contains general scatterometer data handling and wind processing routines that are also used by

SDP, available through the NWP SAF (Vogelzang et al., 2010). OWDP is to a large extent based on SDP.

In the case of L2A HDF5 input data, OWDP averages the slice backscatter data to Wind Vector Cell (WVC) level:

$$\sigma^0 = \frac{\sum_{S} \alpha_S^{-1} \sigma_S^0}{\sum_{S} \alpha_S^{-1}}$$

where σ^0 is the WVC backscatter, σ^0_S is the slice backscatter and α_S is the slice K_p-alpha. The weights α_S^{-1} were found to be proportional to the estimated transmitted power contained in a slice and thus the above weighting relates to a summation over backscattered power. The Sigma0 Quality Flag present in the HDF5 data is evaluated and slice data with one of the following flags set are skipped:
- Sigma0 is poor
- Kp is poor
- Invalid footprint
- Footprint contains saturated slice

The WVC K_p values α, β and γ are computed from the slice K_p's as

$$\alpha = \left(\sum_{S} \alpha_S^{-1} \right)^{-1}, \quad \beta = \left(\sum_{S} \beta_S^{-1} \right)^{-1}, \quad \gamma = \left(\sum_{S} \gamma_S^{-1} \right)^{-1},$$

the WVC received power P is computed from the slice received power as

$$P = \sum_{S} P_S, \quad P_S = 2 \cdot SNR_S / \beta_S$$

and the WVC SNR is calculated as

$$SNR = \beta \cdot P / 2.$$

Now $K_p^2 = \alpha + \beta/SNR + \gamma/SNR^2$ is obtained for each WVC view.

ECMWF NWP model sea surface temperature and land-sea mask data are used to provide information about possible ice or land presence in the WVCs. WVCs with a sea surface temperature below 272.16 K (-1.0 °C) are assumed to be covered with ice and no wind information is calculated. Land presence within each WVC is determined by using the land-sea mask available from ECMWF. The weighted mean value of the land fractions of all model grid points within 80 km of the WVC centre is calculated. The weight of each grid point scales with $1/r^2$, where r is the distance between the WVC centre and the model grid point. If this mean land fraction value exceeds a threshold of 0.02, no wind retrieval is performed.

Subsequently, OWDP inverts the WVC backscatter data to ambiguous wind solutions using the NSCAT2 Geophysical Model Function (GMF). No winds have yet been computed in the outer parts of the swath where only VV-polarised outer beam data are available, WVC numbers 1-4 and 33-36. The Multiple Solution Scheme, where 144 wind solutions with their associated probabilities are considered (see Vogelzang et al., 2010), is applied. A basic quality control step is done after the wind inversion; all WVCs in which the wind solution closest to the NWP background wind has a Maximum Likelihood Estimator (MLE) value above a certain threshold are rejected. This procedure has been carefully tuned for SeaWinds and proves very effective for rain decontamination (Portabella and Stoffelen, 2001, 2002a,b). The OSCAT threshold is set such that the procedure rejects approximately 5% of the WVCs, a rejection rate which is the same as obtained in SDP for the SeaWinds data. Ambiguity removal is performed in order to select the appropriate wind solution and ECMWF model forecast (3 to 18 hours) winds are used to initialise the ambiguity removal step.

In the case of L2B HDF5 input data; our analysis uses the ISRO-selected winds (Wind_speed_selection, Wind_direction_selection) rather than the ISRO ambiguities (Wind_speed, Wind_direction, WVC_selection) from the input. The ISRO-selected winds compare slightly better to the ECMWF model winds. The backscatter data in the constructed ISRO L2B BUFR output are missing in this case.

EVALUATION OF BACKSCATTER DATA

As a first step, the slice backscatter data present in the HDF5 L2A files have been evaluated. Figure 1 shows a plot of the slice KpA (α_S) versus the slice Sigma0 (σ^0_S). Since α_S depends on the slice bandwidth and on the transmit pulse width only (see section 5.1 in Padia, 2010), the distinct levels in the plot must correspond to different slice types in the egg footprint. Similar plots were made for β_S (middle pane of Figure 1) and γ_S (not shown here). One striking feature in the plot is that for slices corresponding to low α_S or β_S values, no low σ^0_S values (below approximately -50 dB) occur.A4 page in Arial 10 point font size justified, 2.5 cm margin on either side, 3 cm margin each for top and bottom, line spacing single, single-column layout (text runs from left margin through to right margin, NO split into two or more columns), one clear line between paragraphs. Do not use additional footers or headers.
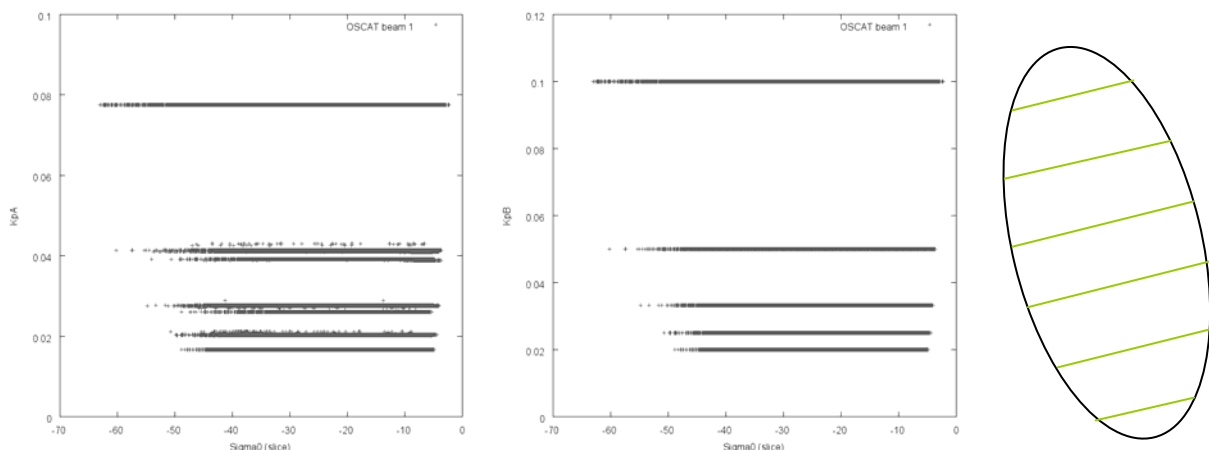

Figure 1: **Slice KpA versus slice Sigma0 (left), slice KpB versus slice Sigma0 (middle) and schematic drawing of slices forming an "egg" (right).**

As a next step, we plotted collocated σ^0_S values corresponding to the same WVC, but with different values of α_S, i.e. originating from different parts of the egg footprint, see Figure 2. This plot is made for the inner forward beam (HH), but the other beams show similar results. Since the backscatter data are from (almost) the same location on the Earth, a linear relation between the data along both axes is to be expected. However, in the scatter plot (left in Figure 2) it looks as if the σ^0_S from different slice types are biased with respect to each other, especially for low backscatter values. This bias does not appear however when we plot the same slice backscatter values in a contoured histogram (right in Figure 2). There is no bias as can be seen from the red curve in the bottom right pane.
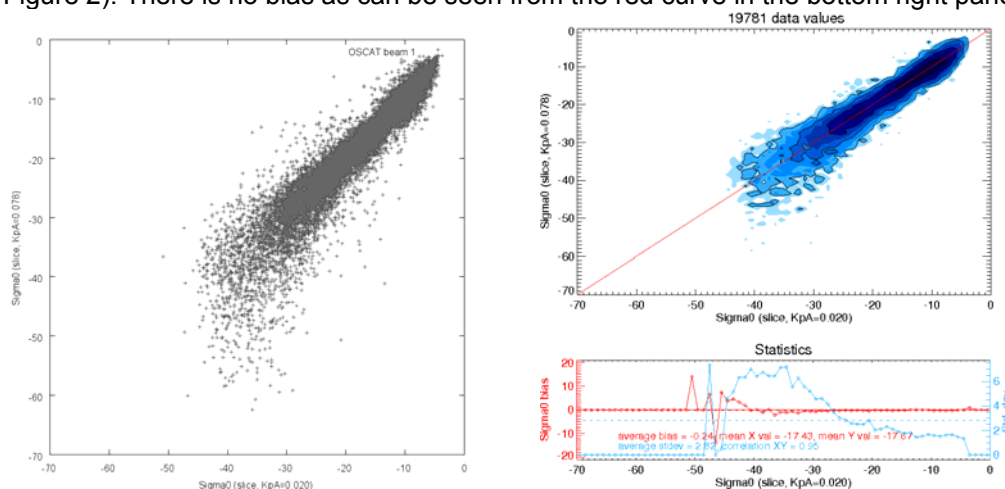

*Figure 2:*Scatter plot of slice Sigma0 corresponding to KpA of 0.078 versus slice Sigma0 corresponding to KpA of 0.020 (left) and the same plotted as contoured histogram.
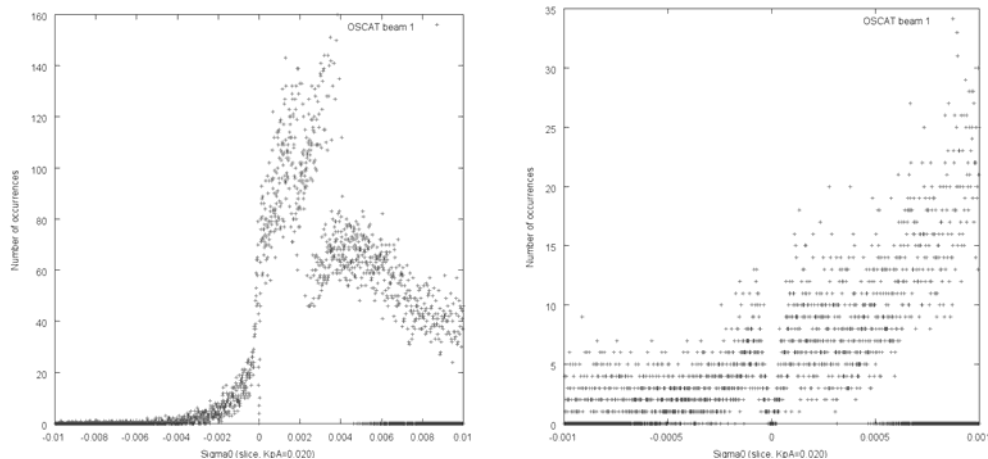
Figure 3: probability density function of slice backscatter values corresponding to slice KpA of 0.020 around zero. The scatter plots show the number of occurrences versus the slice Sigma0 on a coarse (left) and finer (right) scale. A Sigma0 of 0.01 corresponds to -20 dB, a Sigma0 of 0.0005 to -33 dB.

The behaviour of the slice backscatter values around zero is shown in more detail in Figure 3, where probability density functions (PDFs) of the $\sigma^0{}_S$ are shown on different horizontal scales. The left hand side plot shows an increasing distribution towards zero, followed by a decrease below 0.002. The decreasing trend is clearer in the right hand side plot. This is all to be expected, but two phenomena are striking: the dip in the distribution very close to zero and the fact that the distribution extends to negative values up to -0.005 and lower. The distribution for backscatter data corresponding to a KpA of 0.078 (not shown) show similar behaviour, except for the dip around zero which is replaced by a peak. From the PDFs we conclude that there may be an issue with the level 0 to level 1 processing for low $\sigma^0{}_S$ values.

Figure 4 shows the PDF of the WVC σ^0 values as computed by OWDP. The results of the slice backscatter analysis are confirmed and it is clear that there is a cut-off below -40 dB which will influence the wind inversion results, especially in low wind regions.
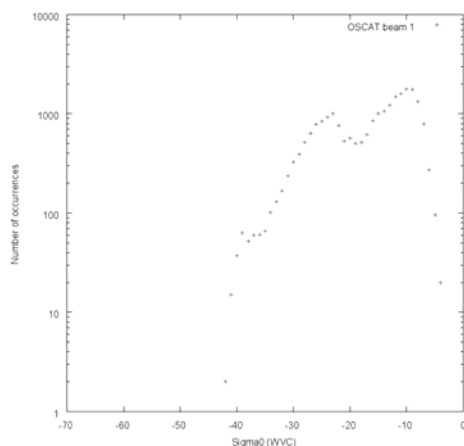
Figure 4: probability density function of WVC backscatter values. The Sigma0's are on a dB scale.

In order to assess the quality of the instrument backscatter measurements, we computed expected WVC σ^0 values from the ECMWF model winds. The NSCAT2 GMF, used successfully in SDP for wind retrieval, was applied to the collocated model winds. These simulated backscatter data are plotted against the measured WVC σ^0 values in Figure 5. It is clear from the left plot that the median of the contour is not along the diagonal for lower backscatter values. In order to correct for this we applied a simple linear σ^0 correction below -27 dB. This results in a better linear relationship between expected and measured σ^0, but the PDF is cut off at even higher backscatter values of approximately -35 dB.

Note that in the averaging process for the computation of the WVC backscatter values, the "Negative Sigma0" flag in the slice Sigma0 Quality Flag information was neglected, i.e., all slice σ^0 values are considered to be positive. When this flag is taken into account, in many cases negative σ^0 values occur on WVC level leading to a high fraction of WVCs where no winds can be computed. This is consistent with the results shown in Figure 3 in the previous section. In the latest L2A version from ISRO (Sept. 2011) the amount of negative backscatter values is much reduced. Moreover, the backscatter correction is limited to an overall -1 dB for both VV and HH.
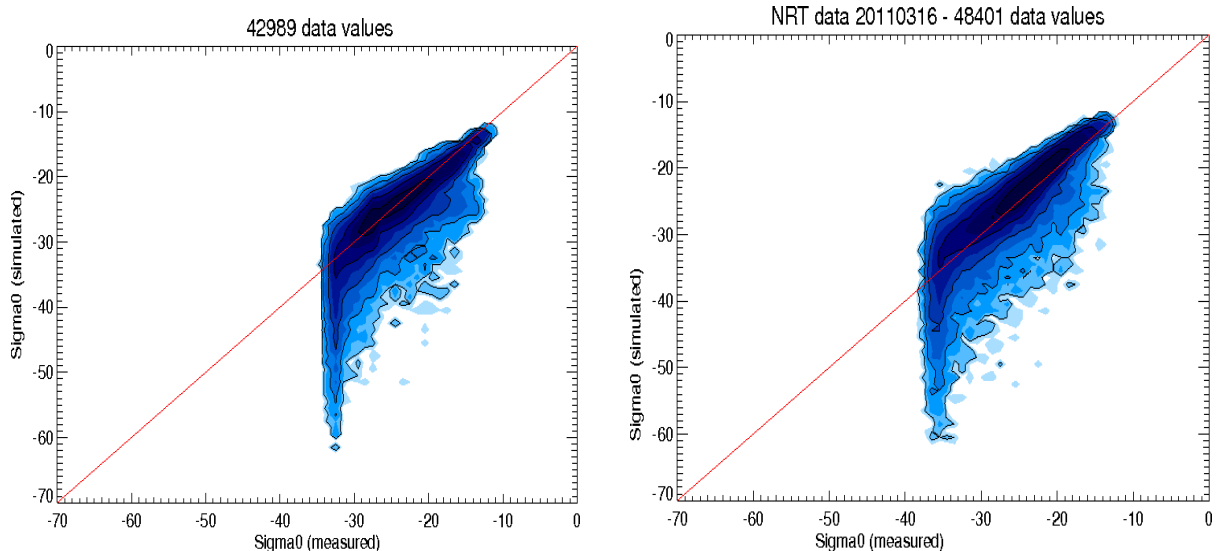

Figure 5: **contour plots of simulated WVC backscatter against measured WVC backscatter for the inner forward beam (HH), with correction in v2010 (left) and without (right) Sigma0 correction in v2011 (see text).**

EVALUATION OF WINDS

The contoured histograms in Figures 6 and 7 show statistics of the wind speed, wind direction (with respect to wind blowing from the North), and u (eastward) and v (northward) wind components. The scatterometer winds are compared with ECMWF forecast winds (3 to 18 hours ahead); the model winds are interpolated with respect to time and location. The ISRO L2B product wind speed (Figure 6, top left panel) is clearly biased low for wind speeds below approximately 5 m/s. The winds created with OWDP have less wind speed bias, but show a cut off below 3 m/s. This is due to the problematic (corrected) backscatter distribution, containing no σ^0 values below -40 dB.

The u and v wind component standard deviations for the ISRO L2B product are 1.87 and 1.76 m/s, respectively. For the OWDP product the u and v wind component standard deviations are 1.62 and 1.55 m/s, respectively, i.e., the OWDP product compares better to ECMWF winds than the IL2B product. For the OSI SAF SeaWinds 25-km product, we found standard deviations of 1.28 and 1.40 m/s for a comparable data set, i.e., considerably lower values.

The Oceansat-2 wind data have also been compared with in situ winds from moored buoys. The buoy winds are distributed through the Global Telecommunication System (GTS) and have been retrieved from the ECMWF MARS archive. The buoy data are quality controlled and (if necessary) blacklisted by ECMWF (Bidlot et al., 2002). We used a set containing approximately 150 moored buoys spread over the oceans (most of them in the tropical oceans and near Europe and North America) which are also used in the buoy validations that are routinely performed for the OSI SAF wind products (see the links on http://www.knmi.nl/scatterometer/osisaf/). A scatterometer wind and a buoy wind measurement are considered to be collocated if the distance between the WVC centre and the buoy location is less than the WVC spacing divided by √2 and if the acquisition time difference is less than 30 minutes. The buoy winds are measured hourly by averaging the wind speed and direction over 10 minutes. The real winds at a given anemometer height have been converted to 10 m equivalent
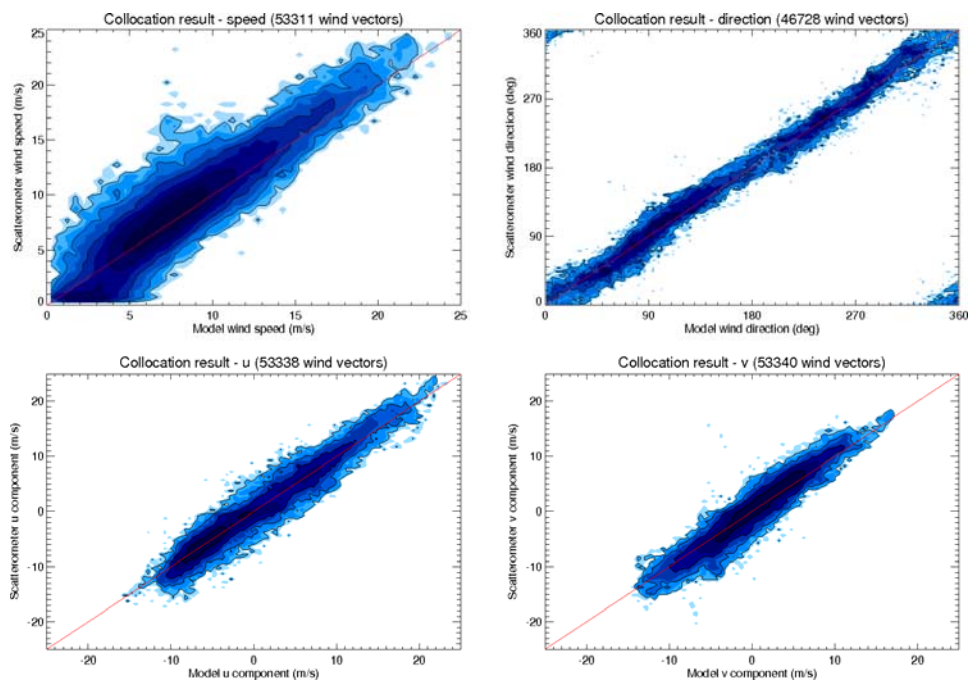
Figure 6: **contoured histograms of Oceansat-2 winds from the ISRO level 2b product versus ECMWF forecast winds for 4 orbits (638-641) on 6 November 2009.**
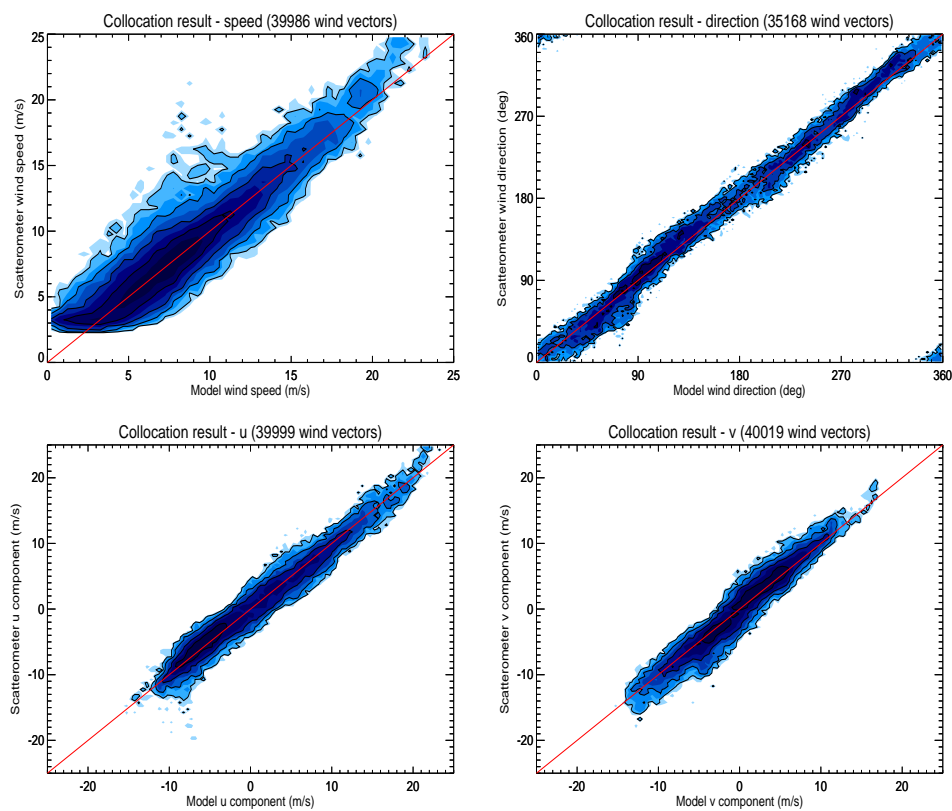
Figure 7: **contoured histograms of Oceansat-2 winds from OWDP versus ECMWF forecast winds for 4 orbits (638-641) on 6 November 2009. A sigma0 correction has been applied (see text). The lower plot PDF statistics are within OSI SAF wind quality requirements.**

neutral winds using the LKB model (Bidlot et al., 2002, Liu et al., 1979) in order to enable a good comparison with the 10 m scatterometer winds (Portabella and Stoffelen, 2009).The buoy validation results in terms of standard deviations of wind speed, wind direction and *u* and *v* components are summarised in Table 1. From the first two lines, it appears that more buoys are used in the OWDP collocations than in the ISRO L2B product collocations (158 versus 131 buoys). This is due to the fact that in the ISRO L2B product a quite conservative land mask is used and hence many buoys in coastal areas are ruled out. In the OWDP processor we apply land screening based on an ECMWF land-sea mask which is less strict, see section 2. Another difference between the ISRO L2B and OWDP products is that the outer swath is not processed in OWDP, resulting in a lower number of collocations.

In order to compare a shared set of winds from both products, the data sets have been collocated; see lines (3) and (4) in Table 1. When we compare line (1) with (2) and line (3) with (4), respectively, it appears that the OWDP winds compare better to the buoys in terms of speed and wind component standard deviations. The ISRO winds compare better in terms of wind direction standard deviations. Another feature arising is that both the ISRO winds and the OWDP winds improve when the data sets are collocated: compare line (3) with (1) and line (4) with (2), respectively. The collocated data set only contains winds that have passed both the ISRO and the OWDP quality control steps. Apparently both quality control algorithms have a good skill to reject bad quality winds and in this respect they are supplementary.

Since we know that there is an issue with the backscatter values below approximately -40 dB, we also computed the statistics for WVCs containing wind speeds of 6 m/s and higher, i.e. leaving out the data with low σ^0 values. The results are shown in lines (5) and (6) of Table 1. It appears that the *u* and *v* statistics of the ISRO L2B product get worse (compare line (3) with (5)), but that the statistics of the OWDP winds improve (compare line (4) with (6)). Note that these OWDP winds achieve a vector-RMS difference with buoys below 3 m/s. Buoy vector errors are typically 1.6 m/s (Vogelzang et al., 2010), which leaves the OWDP vector error to about 2.5 m/s, just within the OSI SAF wind quality requirement.

Oceansat-2 50-km product standard deviations	Speed (m/s)	Direction (degrees)	*u* (m/s)	*v* (m/s)
(1) ISRO L2B, 131 buoys	1.46	23.56	2.38	2.35
(2) OWDP, 158 buoys	1.37	23.91	2.27	2.20
(3) ISRO L2B, 130 buoys, OWDP collocated	1.38	22.17	2.29	2.18
(4) OWDP, 130 buoys, ISRO L2B collocated	1.25	22.82	2.11	2.06
(5) ISRO L2B, OWDP collocated, ≥ 6 m/s	1.34	19.40	2.41	2.30
(6) OWDP, ISRO L2B collocated , ≥ 6 m/s	1.33	16.67	2.02	2.12

Table 1: **Oceansat-2 buoy validation results over November 2009 – May 2010.**

In the version of OWDP winds based on new ISRO L2A data (v2011) several further improvements in the winds are seen (with respect to v2010):
- Speed bias much reduced
- Improved wind direction
- Reduced wind speed cut-off, now at ~2 m/s
- Vector RMS difference against ECMWF 1.9 m/s (as SDP25)

This vector RMS difference, including the ECMWF model error, is lower than the threshold OSI SAF Vector RMS error requirement of 2 m/s. As such, the OWDP winds fulfill EUMETSAT requirements.

CONCLUSIONS

The assessment of the Oceansat-2 backscatter data reveals that the data quality is promising and that an initial processing issue with the low σ^0 values which prevents a proper wind computation in locations with low winds has now been much improved. A 1 dB σ^0 bias with respect to QuikSCAT for all backscatter values can be corrected in a fairly simple way.

The ISRO L2B wind data quality is reasonable, although the wind component standard deviations with respect to ECMWF model winds and in situ buoy winds are higher than 2 m/s; which leave the wind component errors above the EUMETSAT OSI SAF specification limit. Winds computed with OWDP from the L2A product are generally of better quality and within the OSI SAF quality requirements.

Acknowledgements

References

Bidlot J., D. Holmes, P. Wittmann, R. Lalbeharry, and H. Chen (2002), Intercomparison of the performance of operational ocean wave forecasting systems with buoy data, *Wea. Forecasting*, vol. **17**, 287-310

Leidner, S.M., Hoffman, R.N. and Augenbaum, J. (2000), SeaWinds Scatterometer Real-Time BUFR Geophysical Data Product User's Guide, Version 2.3.0.

Liu, W.T., K.B. Katsaros, and J.A. Businger (1979), Bulk parameterization of air-sea exchanges of heat and water vapor including the molecular constraints in the interface, *J. Atmos. Sci.*, vol. **36**, 1979.

Padia, K. (2010), Oceansat-2 Scatterometer algorithms for sigma-0, processing and products format, Version 1.1, April 2010.

Stoffelen, A. (2008), Research and Development in Europe on the Global Application of the OceanSat-II Scatterometer, *Announcement of Opportunity (AO) proposal submitted to ISRO on 30 June 2008.*

Portabella, M. and A.C.M. Stoffelen (2009), *On Scatterometer Ocean Stress,* J. Atm. Oceanic Technol., 26, 2, 368-382, doi:10.1175/2008JTECHO578.1

Portabella, M. and A. Stoffelen (2002a), *A comparison of KNMI Quality Control and JPL Rain Flag for SeaWinds,* Canadian Journal of Remote Sensing, , 28, 3, 424-430.

Portabella, M. and A. Stoffelen (2002b), *Characterization of Residual Information for SeaWinds Quality Control,* IEEE Transactions on Geoscience and Remote Sensing, , 40, 12, 2747-2759, doi:10.1109/TGRS.2002.807750.

Portabella, M. and A. Stoffelen (2001), *Rain Detection and Quality Control of SeaWinds,* J. Atm. Oceanic Technol., , 18, 7, 1171-1183.

Vogelzang, J., J. de Kloe, M. Portabella, A. Stoffelen, A. Verhoef and J. Verspeek (2010), SDP User Manual and Reference Guide version 2.1, *NWPSAF-KN-UD-002, EUMETSAT*